Research Article

Zheng Lv, Zhou-Yi Yang, Jian-Yu Zhang, Xue-Tong Li, Peng Ji, Qian Zhou*, Xi-Liang Zhang, and Yin-Dong Shi

Numerical simulation and experimental research on cracking mechanism of twin-roll strip casting

https://doi.org/10.1515/htmp-2022-0251
received July 16, 2022; accepted November 02, 2022

Abstract: Based on the three-dimensional field of molten pool and twin-roll strip casting experiments, this work verified the cracking mechanism of the strip by establishing mathematical model and rolling experiments. The results showed that due to the instability of the thermophysical field of the molten pool and the inconsistency of kiss curve height, the newly solidified strip will undergo incompatible deformation through the rolling. The stress concentration will appear around the large reduction area and then form slip bands. When plastic strain exceeds the limit of the metal, the oblique cracks will appear in the slip bands periodically or completely penetrate the strip. In addition, tensile cracks could also be produced by incompatible deformation. Therefore, keeping the uniformity and stability of the thermal physical field in molten pool is the key factor to restrain cracks.

Keywords: twin-roll strip casting, mathematical model, kiss curve, oblique crack

1 Introduction

The twin-roll strip casting (TRC) uses a pair of relatively rotating rollers as crystallizers to solidify and roll the liquid metal to a strip in a short time [1,2] (Figure 1). However, this technology is not mature enough [3,4]. The crack problem has a very harmful effect on the mechanical properties of the strip [5]. However, the causes of cracks are complex and variable, such as chemical composition, thermal stress, grain dislocation and other factors [6,7].

Harada et al. [8] found that higher casting speed and higher cooling rate can reduce the occurrence rate of cracks on the strip surface effectively. El-Bealy [9] also proved that the interdendritic crack is related to cooling conditions and strain distribution. Xu et al. [10] believed that the crack sources mainly appear at the grain boundary of the strips' surface and propagate along the grain boundary, and the rapid solidification of small-size grains would be helpful for the crack propagation. However, Hu et al. [11] researched high silicon steel and found that the number of oblique and longitudinal cracks are far more than the transverse cracks on the strip surfaces, and the transverse and longitudinal cracks have caused transgranular fracture, he also pointed out that the uneven heat transfer is the main factor leading to surface cracks. Kim et al. [12] reported that the thermal conductivity of semi-solid area in molten pool is so weak, which leads to the interlayer cracks. He also pointed out that the rolling force should be increased to move the semi-solid area up, which could restrain the cracks. However, Zang et al. [13] believed that if the rolling force is increased, the deformation of strip will be enlarged, and the as-cast strip will be prone to cracking more easily. Therefore, the rolling force cannot be excessive during the TRC process.

In fact, most of the strip cracks are oblique cracks (Figure 3). So the crack problems are difficult to be solved in the two-dimensional field [13]. In the three-dimensional field, this work studies the cracking mechanism through experiments and mathematical models, based on the molten pool temperature field, material deformation and cracking theory.

2 Analysis of TRC cracks

Based on the $\Phi 265 \times 120$ strip casting mill (Figure 2) with copper alloy crystallization rollers, the thin casting strip

* **Corresponding author: Qian Zhou,** School of Materials Science and Engineering, Hebei University of Engineering, Handan 056038, China, e-mail: 491056685@qq.com
Zheng Lv, Zhou-Yi Yang, Jian-Yu Zhang, Xue-Tong Li, Peng Ji: School of Mechanical and Equipment Engineering, Hebei University of Engineering, Handan 056038, China
Xi-Liang Zhang, Yin-Dong Shi: School of Materials Science and Engineering, Hebei University of Engineering, Handan 056038, China

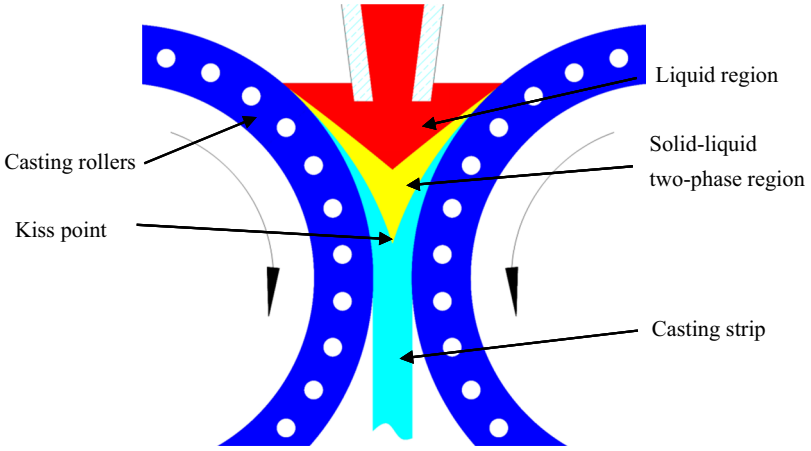

Figure 1: The TRC processing.

Figure 2: The TRC mill.

has been carried out. As shown in Figure 3, cracks often occur on casting strip forming crack bands (such as edge crack bands). In order to study the causes of the cracks, the fracture morphology of the cracks was analyzed by stereomicroscope (Figure 4). The results show that there is a certain thickness of oxide layer on the fracture surface, which indicates that the crack was generated in the high temperature period, which is similar to the experimental results of Hu et al. [14].

However, there are obvious directional plastic deformation marks on the oblique crack fracture, and the flow traces are basically parallel to the crack direction. It means that the crack in this region grew by the action of shear force mainly. So these oblique cracks are sliding mode cracks, and the crack band is shear slip band. In general, slip band is hard to be formed during the solidification, so it should be produced during rolling deformation.

Although the kiss point (KP) and solidification interface can be obtained clearly in the two-dimensional field, due to the uneven distribution of flow and temperature in the molten pool, it is difficult to get a parallel and smooth kiss curve in the three-dimensional field. As shown in Figure 5a, the KP may be moving up the area which has low flow rate or efficient heat transfer (such as point A).

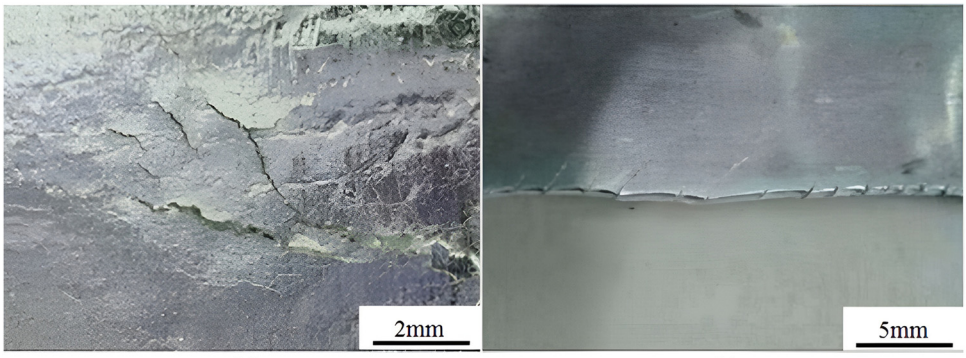

Figure 3: The crack of cast-rolling strip: (a) Surface oblique cracks and (b) edge cracks.

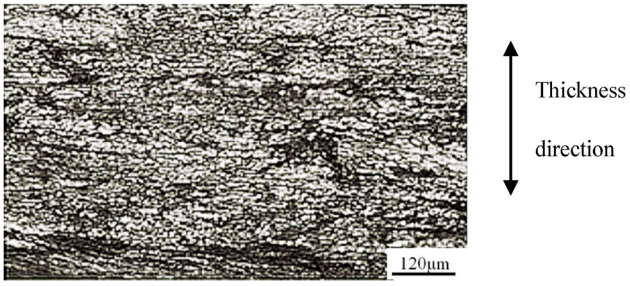

Figure 4: Fracture morphology of the oblique crack.

On the contrary, the KP will decline where there is large flow rate or weak heat exchange (such as point B) [15].

So different positions correspond to different rolling reductions (Figure 5b). The rolling reduction (Δh_N) is as follows:

$$\Delta h_{\mathrm{N}} = 2R\left[1 - \cos\left(\arcsin\frac{l_{\mathrm{N}}}{R}\right)\right], \quad (1)$$

where R is the radius of crystallization roller, l_{N} is the height of KP. So, it can be seen that the rolling reduction only depends on the height of KP. So the deformation and cracking mechanism of casting strip could be proposed as Figure 5c. Since the roll gap is a fixed value, the raising of KP position means the increase in rolling deformation, so the rolling area will produce incompatible deformation and form slip bands which is easy to crack.

3 Rolling experiment of cracks

In order to verify the cracking mechanism in this study, rolling experiments of cracks were designed by using as-cast A3003 aluminum alloy slab with uneven thickness (Figure 6). To ensure that the experimental conditions are close to the twin-roll casting process, the alloy slab had been heated to 600°C (close to solidus temperature) for rolling, the specific experimental parameters are shown in Table 1.

As shown in Figure 7, the experimental results show that the metal strip changes from the rectangular shape into a long polygon, the deformation is incongruous. The central thick area mainly endures bearing stress, which is much larger than the thin areas. The thick area material flows transversely and extrudes the surrounding region, resulting in forming complex shear slip bands near the juncture between thick and thin areas. Figure 7 also shows that there are obvious oblique macro cracks near the junctures, which are distributed periodically or completely penetrable. In addition, many tiny micro-cracks also appear in the slip area.

The TRC technology belongs to sub-rapid solidification, the liquid metal solidifies so fast that the solidification defects cannot be filled in time. So there are many defects in casting structure frequently, the intermolecular dislocation defects are numerous, and the crack sources

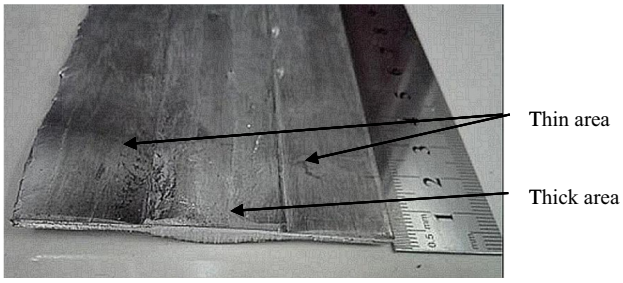

Figure 6: As-cast 3003 aluminum alloy slab.

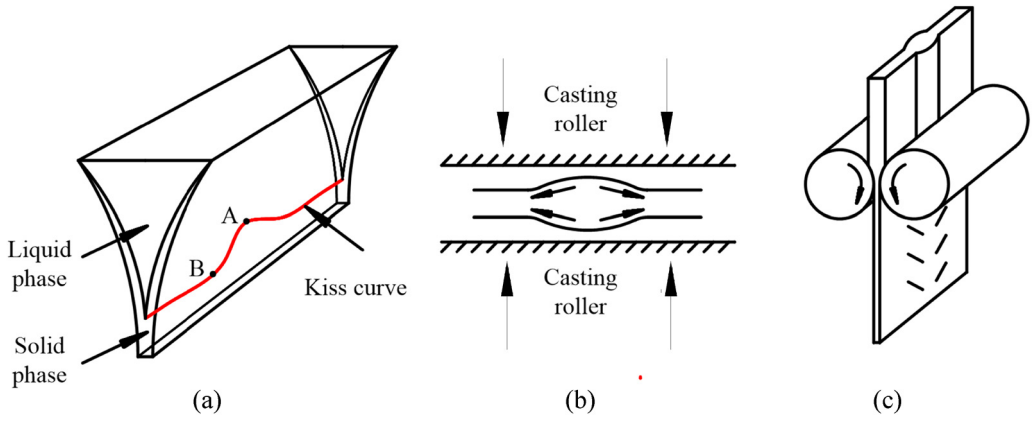

Figure 5: The mechanism of casting strip crack: (a) uneven kiss curve of molten pool; (b) material deformation tendency by rolling; (c) traces of material deformation cause cracks.

Table 1: Crack experimental parameters of strip rolling

Project	Parameter	Project	Parameter
Initial rolling temperature	600°C	Experiment material	A3003 (as-cast)
Roller diameter	265 mm	Thickness of slab thick area	4.5 mm
Roll gap	2.0 mm	Width of slab thick area	30 mm
Rolling speed	30 mm·s^{-1}	Thickness of slab thin area	2.1 mm

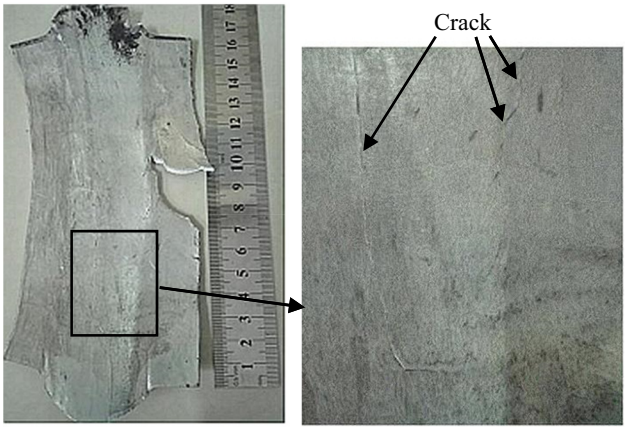

Figure 7: Crack experimental results by rolling.

may occur randomly. But the cracks are mainly concentrated in the transition area between thick and thin areas. The main reason is that the material in the transition area not only has lots of longitudinal deformations, but also has a large number of transverse deformations, so that the accumulation strain is larger than other areas. According to crack theory, the slip bands easily generate stress concentration at the intermolecular dislocation defects, forming many tiny micro-cracks first. Then, the micro-cracks continue to expand and interconnect to form macro-cracks under external pressure. The incompatible deformation and deformation potential energy will promote the slip cracks' growth [16], but the crack growth can release a part of potential energy. When the two effects reach equilibrium, the cracks will stop growing. However, the incompatible deformation and deformation potential energy may accumulate on the slab surface again with the rolling, until a new crack appeared. Therefore, the oblique cracks of the experimental strips will be periodically distributed, and the cracks may penetrate strips completely when deformation potential energy is excessive [17].

In addition, the material structure is mainly high temperature solid solution when the metal is just solidifying during the casting process. The plastic and slip property of the high temperature metal is unstable relatively, and easy to be changed by the temperature, which makes the processing more complex. Therefore, the incongruous deformation of the material is the main factor to produce cracks.

4 Mathematical model of strip casting and cracking

4.1 Constitutive equation of the materials

Based on the assumption of this work, the mathematical model of TRC cracks is established. The strength of the metal is weak when the temperature is little lower than the solidus temperature, so the metal is elastic viscoplastic material [18]. The constitutive equation is as follows:

$$\begin{cases} \varepsilon_{ij} = \dfrac{1+\nu}{E}\sigma_{ij} - \dfrac{\nu}{E}\sigma_{kk}\delta_{ij} + \lambda s_{ij} \\ \lambda = \dfrac{\lambda_{\mathrm{p}}}{1+\eta\lambda_{\mathrm{p}}} = \dfrac{1}{\eta}\left[1 - \dfrac{F(\overline{\varepsilon}_{\mathrm{p}})}{\sigma}\right] \end{cases}, \tag{2}$$

where ε is the strain of the metal; σ is the stress; ν is Poisson's ratio; i and j are the direction vectors; E is the Young's modulus; λ is the viscoplastic factor, which depends on the viscosity and Mach number of the metal; λ_{p} is the plastic flow factor; $F(\overline{\varepsilon}_{\mathrm{p}})$ is the plastic loading function; and η is the viscoplastic factor of the metal.

4.2 Heat transfer model

The influence of contact stress on interface heat transfer is very obvious. Liu et al. [19] presented a high precision heat transfer theory for aluminum alloy.

$$h = h_{\mathrm{a}} + h_{\mathrm{c}}, \tag{3}$$

where h_{a} represents the heat transfer across the air gap with zero pressure and typically has a low value, h_{c} represents the contact under pressure between two solid surfaces.

$$h_c = \alpha \frac{K_{st} N_P}{R}, \tag{4}$$

where α is a model parameter, K_{st} is the harmonic mean thermal conductivity of the contact solids, R is the root mean square of surface roughness of the contact solids and N_P is a pressure-dependent parameter.

4.3 Crack propagation theory

As shown in Figure 8, it is assumed that point O is the original position of the shear crack and the crack surface is subjected to a pair of tangential stresses q, the crack is growing along direction ξ with the velocity $v(y = 0)$. And the stress of the area far away from the crack is relatively small and can be ignored. So, the cracking process can be considered as semi-infinite crack model. For point O, the stress intensity factor K_{II} is

$$K_{II} = \lim_{\xi \to 0^+} \sqrt{2\pi\xi}\,\sigma_{xy}(\xi, \pm 0) = \frac{q}{2}\sqrt{\frac{2}{\pi l}}. \tag{5}$$

The propagation conditions of sliding crack are calculated as follows:

$$K_{II} \geq K_c, \tag{6}$$

where K_c is the limit factor of the materials. In addition, the crack length (l) increases with the crack growth, so K_{II} will decrease and cracks can stop propagating at some time.

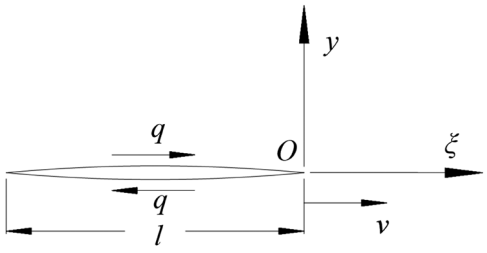

Figure 8: Force analysis of crack propagation.

4.4 Numerical simulation model

An equal scale mathematical model corresponding to the experimental conditions is established (Figure 9), and mesh encryption is carried out at key locations such as the junction area of the model. For the quasi-static problem of rolling, the explicit algorithm is used to analyze the deformation distribution and deduce the cracking trend and change. The process conditions of numerical simulation model are identical with the crack experiment of strip rolling (as shown in Table 1).

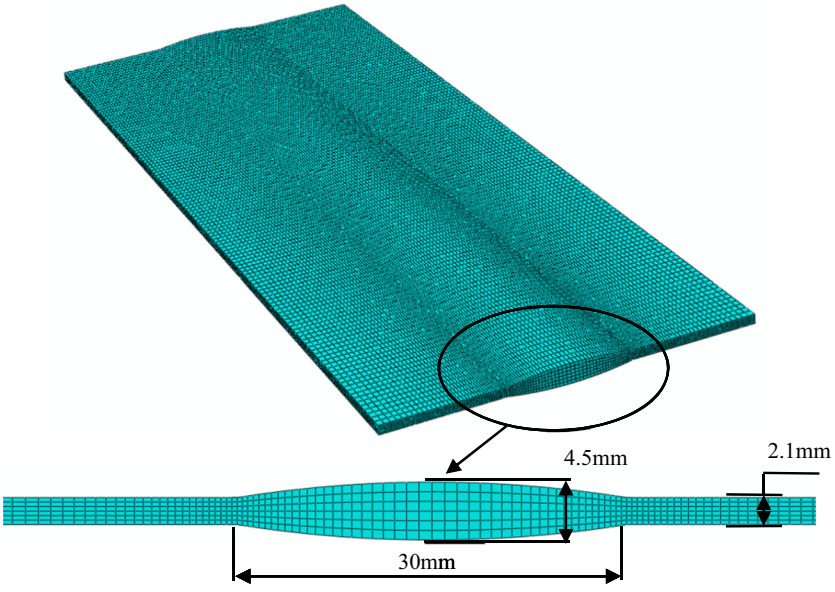

Figure 9: The mesh of mathematical model.

5 Result analysis of mathematical model

5.1 Result analysis of simulation model

The temperature field distribution shows differences between thin and thick areas (Figure 10). Because heat transfer is associated with contact stress, the thick area has larger contact area, contact stress and heat transfer. The temperature of the thick area is about 36.3°C lower than others, which means that the thick area metal has high stress intensity to extrude the surrounding areas. In addition, the temperature difference may lead to uneven shrinkage through subsequent processing, which will promote the crack propagation.

After rolling, the metal with thin areas is subjected to tension, but thick area is under compressive force (Figure 11), slip bands emerge near the junction. So, the Tresca stress is the key parameter for cracks. Figure 11 also shows that periodical Tresca stress emerges at the slip bands. According to crack theory, if $K_{II} \geq K_c$, the oblique cracks in the experimental strip may be distributed at the slip bands periodically, which is basically consistent with the experimental results (as shown in Figure 7). It can be seen that the cracks are closely related to the temperature distribution in the molten pool, and the distribution of temperature could also be reflected by the crack trace of the strip.

The plastic strain of slip bands is much larger than others (Figure 12), because the uneven deformation can extrude the material to flow transversely. Slip bands are subjected to not only longitudinal deformation but also transverse deformation; therefore, the plastic strain is concentrated at the slip bands, which tends to crack, or even break. In addition, the cracks will further grow to small reduction area because of its tension, which is similar to the experimental results.

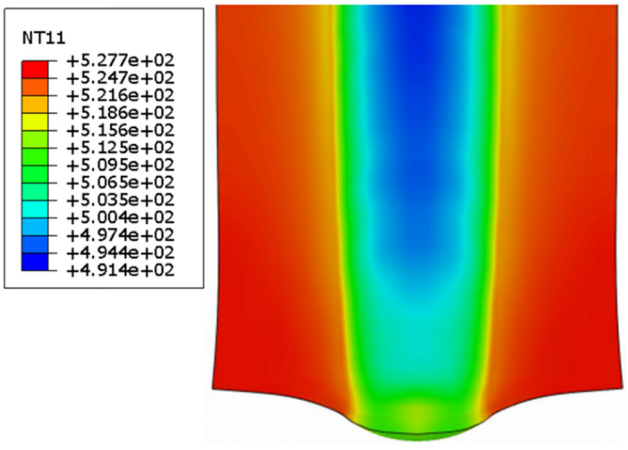

Figure 10: Temperature distribution of simulation model (°C).

5.2 Analysis of non-uniform rolling reduction

This work further studies the effect of different rolling reductions on temperature and strain. This work set the thickness of center area as 3.3, 3.9 and 4.5 mm (altitude differences of kiss curve are 9.5, 12.2 and 14.5 mm), and the same boundary conditions of Table 1. The results of temperature and strain are shown in Figures 13 and 14.

After rolling, thick area temperature is lower than the rest of the areas. With the decrease in the rolling

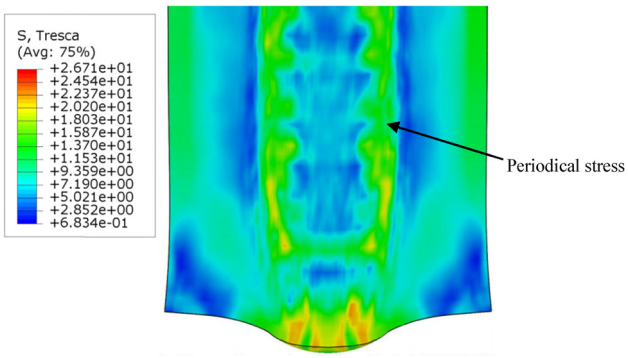

Figure 11: Tresca stress distribution of simulation model (MPa).

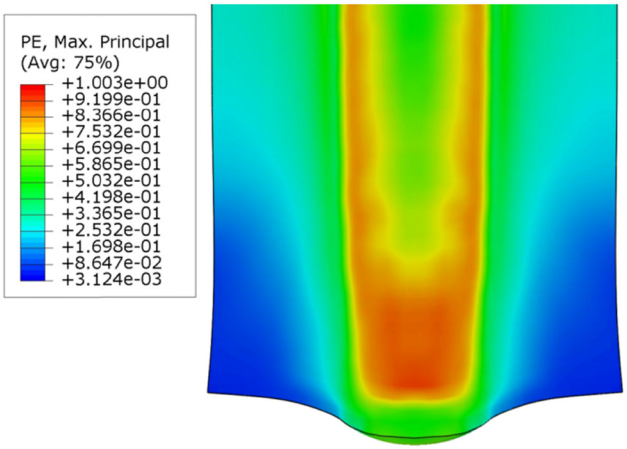

Figure 12: Plastic strain distribution of simulation model.

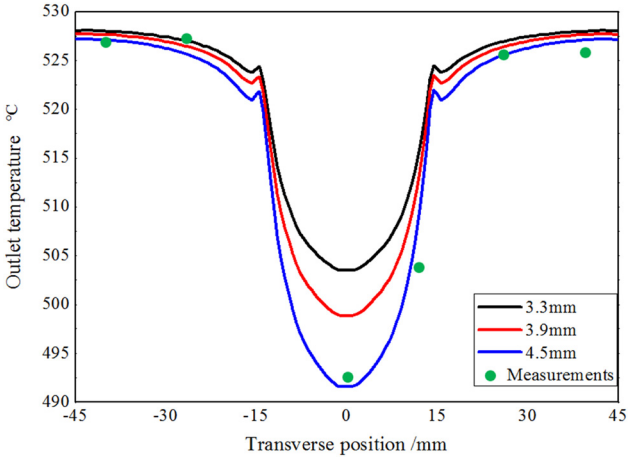

Figure 13: Temperature distribution of strip in transverse direction.

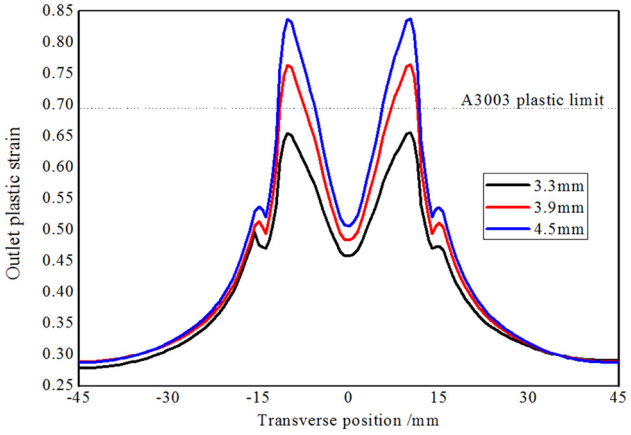

Figure 14: Plastic strain distribution of strip in transverse direction.

reduction, the temperature at the central area increases gradually, while the temperature of thin areas is not changed much, because the rolling reduction has no significant change. However, the strain results show a different trend. The plastic strain of slip area is the maximum, and its distribution is in the shape of "M." The maximum plastic strain increases linearly with the increase in strip thickness, and when the strain exceeds the allowable limit [20] of the metal at high temperature, the slip area will crack first and extend to the thin areas, because the thin areas bear the tensile stress. The amount of uncoordinated deformation is directly determined by the altitude difference of KP curve. Therefore, controlling the stability of KP curve is the key factor to suppress crack generation.

In addition, the higher rolling speed and larger strain rate could reduce the plastic properties of metal, which may increase cracking tendency for some materials with poor plasticity.

6 Conclusion

(1) The main influencing factor of the TRC crack is the thermal physical field. The altitude difference of kiss curve will lead to different rolling reductions and different heat transfer conditions in each area, which will result in uneven structure of the strip. While the small reduction area is subjected to tension, and the large deformation area is under compressive stress after rolling, then slip bands will emerge between the two areas, and the slip bands are easier to crack.

(2) If the stress or plastic strain in the slip bands exceeds the limit of the material, many tiny micro-cracks will appear in the slip bands first. With the increase in the deformation potential energy, these micro-cracks continue to grow and connect with each other, which result in macro-cracks. The macro-cracks will be distributed periodically or penetrated completely and may continue growing to small reduction area because of its tension.

(3) Reducing the altitude difference of kiss curve can suppress the difference in stress, temperature and strain effectively, which reduces the cracking tendency.

Acknowledgements: The authors gratefully acknowledge the fundamental support from the National Natural Science Foundation of China (Grant nos 51804095 and 51904085) and Key Research Project of Higher Education in Hebei Province (ZD2021020).

Funding information: This research was funded by National Natural Science Foundation of China (Grant nos 51804095 and 51904085) and Key Research Project of Higher Education in Hebei Province (ZD2021020).

Author contributions: Zheng Lv: performed the data analyses and wrote the manuscript; Zhou-Yi Yang, Jian-Yu Zhang and Xue-Tong Li: performed the experiment; Peng Ji: modified and polished the manuscript; Qian Zhou: contributed to the conception of the study; Xi-Liang Zhang and Yin-Dong Shi: contributed significantly to analysis and manuscript preparation.

Conflict of interest: The authors state no conflict of interest.

Data availability statement: The data that support the findings of this study are available from the first author and corresponding author upon reasonable request.

References

[1] Zhi, C., L. Ma, W. Jia, X. Huo, Q. Fan, Z. Huang, et al. Dependence of deformation behaviors on temperature for twin-roll casted AZ31 alloy by processing maps. *Journal of Materials Research and Technology*, Vol. 8, No. 6, 2019, pp. 5217–5232.

[2] Lv, Z., Z. Sun, Z. Hou, Z. Yang, X. Zhang, and Y. Shi. Numerical simulation and experimental study on Twin-roll Strip Casting T2 copper alloy. *High Temperature Materials and Processes*, Vol. 41, No. 1, 2022, pp. 1–7.

[3] Ji, C., H. Huang, X. Zhang, and R. Zhao. Numerical and experimental research on fluid flow, solidification, and bonding strength during the Twin-Roll Casting of Cu/Invar/Cu Clad strips. *Metallurgical and Materials Transactions B*, Vol. 51, No. 2, 2020, pp. 1617–1631.

[4] Qian, X., X. Li, Y. Li, G. Xu, and Z. Wang. Microstructure evolution during homogenization and hot workability of 7055 aluminum alloy produced by twin-roll casting. *Journal of Materials Research and Technology*, Vol. 5, 2021, pp. 2536–2550.

[5] Pesin, A. and D. Pustovoytov. Research of edge defect formation in plate rolling by finite element method. *Journal of Materials Processing Technology*, Vol. 220, 2015, pp. 96–106.

[6] Lv, Z., F. S. Du, Z. An, H. Huang, Z. Xu, and J. Sun. Centerline segregation mechanism of twin-roll cast A3003 strip. *Journal of Alloys and Compounds*, Vol. 643, 2015, pp. 643–650.

[7] Xu, M., Z. Li, Z. Wang, and M. Zhu. Computational and experimental study of the transient transport phenomena in a full-scale twin-roll continuous casting machine. *Metallurgical and Materials Transactions, B Process Metallurgy and Materials Processing Science*, Vol. 48B, No. 1, 2017, pp. 471–487.

[8] Harada, H., S. Nishida, E. Masaki, and H. Watari. Casting of high-aluminum-content Mg alloys strip by a horizontal twin-roll caster. *Metallurgical & Materials Transactions B*, Vol. 45, No. 2, 2014, pp. 427–437.

[9] El-Bealy, M. O. Modelling of heat flow and interdendritic crack formation in twin-roll strip casting of aluminium alloys. *Canadian Metallurgical Quarterly*, Vol. 55, No. 1, 2016, pp. 23–44.

[10] Xu, M., G. H. Liu, T. R. Li, B. X. Wang, and Z. D. Wang. Microstructure characteristics of Ti–43Al alloy during twin-roll strip casting and heat treatment. *Transactions of Nonferrous Metals Society of China*, Vol. 29, No. 5, 2019, pp. 1017–1025.

[11] Hu, W. L., Y. X. Zhang, G. Yuan, and G. D. Wang. Crack formation mechanism of high silicon steel during twin-roll strip casting. *Materials Science Forum*, Vol. 898, No. Pt.2, 2017, pp. 1276–1282.

[12] Kim, M. S., Y. Arai, Y. Hori, and S. Kumai. Formation of internal crack in high-speed twin-roll cast 6022 aluminum alloy strip. *Materials Transactions Jim*, Vol. 51, No. 10, 2010, pp. 1854–1860.

[13] Zang, X., L. Liu, and Q. Yang. Cracking possibility evaluation of 304 stainless steel during twin roll casting by 3D simulation. *Journal of Materials Engineering and Performance*, Vol. 30, No. 3, 2021, pp. 2014–2020.

[14] Hu, W. L., Y. X. Zhang, G. Yuan, and G. D. Wang. Crack formation mechanism of high silicon steel during twin-roll strip casting. *Materials Science Forum*, Vol. 4502, 2017, pp. 1276–1282.

[15] Baek, M. S., K. Euh, and K. A. Lee. Microstructure, tensile and fatigue properties of high strength Al 7075 alloy manufactured via twin-roll strip casting. *Journal of Materials Research and Technology*, Vol. 9, No. 5, 2020, pp. 9941–9950.

[16] Huang, Y., B. Xiao, J. Song, H. Zhao, Q. Liu, B. Jiang, et al. Effect of tension on edge crack of on-line heating rolled AZ31B magnesium alloy sheet – ScienceDirect. *Journal of Materials Research and Technology*, Vol. 9, No. 2, 2020, pp. 1988–1997.

[17] Zhang, S. Q., S. H. Jiao, J. H. Ding, Q. F. Zhang, and H. S. Jiang. Simulation study on shear crack of steel plate. *Materials Science Forum*, Vol. 941, 2018, pp. 480–485.

[18] Kroon, M., P. Lindstrm, and M. B. Rubin. An Eulerian thermo-mechanical elastic-viscoplastic model with isotropic and directional hardening applied to computational welding mechanics. *Acta Mechanica*, Vol. 232, No. 1, 2021, pp. 189–218.

[19] Liu, X., K. Ji, O. El Fakir, H. Fang, M. M. Gharbi, and L. Wang. Determination of the interfacial heat transfer coefficient for a hot aluminium stamping process. *Journal of Materials Processing Technology*, Vol. 247, 2017, pp. 158–170.

[20] Chen G., G. Fu, T. Wei, C. Cheng, H. Wang, and J. Wang. Effect of initial grain size on the dynamic recrystallization of hot deformation for 3003 aluminum alloy. *Metals and Materials International*, Vol. 24, No. 4, 2018, pp. 711–719.